



Rheology of rock salt for salt tectonics modeling

Shi-Yuan Li¹ · Janos L. Urai²Received: 14 April 2016 / Published online: 5 October 2016
© The Author(s) 2016. This article is published with open access at Springerlink.com

Abstract Numerical modeling of salt tectonics is a rapidly evolving field; however, the constitutive equations to model long-term rock salt rheology in nature still remain controversial. Firstly, we built a database about the strain rate versus the differential stress through collecting the data from salt creep experiments at a range of temperatures (20–200 °C) in laboratories. The aim is to collect data about salt deformation in nature, and the flow properties can be extracted from the data in laboratory experiments. Moreover, as an important preparation for salt tectonics modeling, a numerical model based on creep experiments of rock salt was developed in order to verify the specific model using the Abaqus package. Finally, under the condition of low differential stresses, the deformation mechanism would be extrapolated and discussed according to microstructure research. Since the studies of salt deformation in nature are the reliable extrapolation of laboratory data, we simplified the rock salt rheology to dislocation creep corresponding to power law creep ($n = 5$) with the appropriate material parameters in the salt tectonic modeling.

Keywords Rock salt rheology · Power law creep · Dislocation creep · Modeling

✉ Shi-Yuan Li
15330011512@163.com

¹ School of Petroleum Engineering, China University of Petroleum, Beijing 102249, China

² Endogene Dynamik, Faculty of Geo-Resources and Materials Technology, RWTH Aachen University, Lochnerstrasse 4-20, 52056 Aachen, Germany

Edited by Yan-Hua Sun

1 Introduction

In recent years, a number of numerical studies about the deformation of salt structures have been published (Schultz-Ela and Jackson 1993; Poliakov et al. 1993; van Keken et al. 1993; Koyi 1996, 1998; Chemia et al. 2008; Chemia and Koyi 2008; Chemia and Schmeling 2009; Li et al. 2009; Ings and Beaumont 2010; Li et al. 2012a). It can be an effective method to study constitutive equations for salt flow based on natural deformation and will deliver reliable reference in salt tectonics and also salt mining engineering. In order to prepare for salt tectonics modeling, the primary problem is what deformation mechanisms of salt can be suitable in the model. In this paper, through the introduction of deformation mechanisms of rock salt and reading previous references about salt creep in laboratories, we have summarized the experimental results and built a database about the strain rate and differential stress relationships. However, direct measurements of rheology at these low rates are not possible, and the rheology of rock salt during long-term deformation in nature is controversial (Li et al. 2012b).

Evaporite rock is mainly composed of carbonates, sulfates, and chlorides. Sodium chlorite (NaCl) is the main chloride, and its mineral form is halite which is also called rock salt. Rock salt influences the salt tectonics and basin evolution because of its specific characteristics including low porosity and permeability, low creep strength and low density (Urai et al. 2008).

The mechanical behavior of rock salt has been investigated in numerous studies during recent decades. The purpose of these studies is to design safe salt mines and develop the design and performance assessment for nuclear waste disposal and oil and gas storage (Wawersik and Zeuch 1986; Cristescu 1998; Hunsche and Hampel 1999).

On a geological time scale, rock salt is a ductile material and behaves like a Newtonian fluid (Schultz-Ela and Jackson 1993; van Keken et al. 1993; Koyi 2001; Gemmer et al. 2004). In recent years, salt mechanics including the theory, experiment and modeling of creep behavior has made progress in China. The research findings have been widely used in layered salt mechanics and engineering (Yang et al. 2009), salt-gypsum layer drilling engineering (Deng 1997; Tang et al. 2004; Yang et al. 2007) and CO₂ geological storage (Liang and Zhao 2007). However, the deformation mechanism of rock salt is relatively less researched in China. The research on the deformation mechanism can lead to a deep understanding of rock salt creep, and a constitutive relation can be built according to microphysics. The creep descriptions based on deformation mechanisms can be used to forecast the geological tectonics and rock engineering stability. It is also relevant to petroleum engineering. For instance, hydraulic fracturing mechanics is an important area of study in petroleum engineering (Zhang et al. 2008; Zhang and Chen 2009, 2010), and the creep properties of rock will also have impacts on fracturing, crack propagation and closure.

2 Deformation mechanisms of rock salt

Two main deformation mechanisms have been investigated in different ways such as laboratory experiments, microstructural investigations and analysis of displacement in actively deforming salt (Fig. 1). One is the dislocation creep mechanism which means crystal defects lead to a dislocation effect. The creep controlled by dislocation mechanisms is widely investigated in laboratory experiments (Carter and Hansen 1983; Carter et al. 1993; Rutter 1983; Urai et al. 1986; Wawersik and Zeuch 1986; Heard and Ryerson 1986; Senseny et al. 1992; van Keken et al. 1993; Franssen 1994; Peach and Spiers 1996; Weidinger et al. 1997; De Meer et al. 2002; Hampel et al. 1998; Brouard and Bérest 1998; Bérest et al. 2005; Ter Heege et al. 2005a, b). The creep equations mainly used in the salt mining industry are based on dislocation creep processes quantified in laboratory experiments (Ottosen 1986; Haupt and Schweiger 1989; Aubertin et al. 1991; Cristescu 1993; Munson 1979, 1997; Jin and Cristescu 1998; Hampel et al. 1998; Hampel and Schulze 2007; Hunsche and Hampel 1999; Peach et al. 2001; Fossum and Fredrich 2002). The steady-state strain rate is related to the flow stress σ using a power law creep (non-Newtonian) equation:

$$\dot{\epsilon}_{DC} = A(\Delta\sigma)^n = A_0 \exp\left(-\frac{Q}{RT}\right) (\sigma_1 - \sigma_3)^n \quad (1)$$

where $\dot{\epsilon}_{DC}$ is the strain rate; $\Delta\sigma = \sigma_1 - \sigma_3$ is the differential stress; $A = A_0 \exp(-Q/RT)$ is the viscosity of the salt; A_0 is a material dependent parameter; Q is the specific activation energy, while R is the gas constant ($R = 8.314 \text{ J mol}^{-1} \text{ K}^{-1}$); and T is the temperature.

The other mechanism is solution-precipitation creep (also called diffusion creep), which means a crystal grain slides along the crystal boundary. It includes pressure solution and dynamic recrystallization processes, and it has a strong relation with water content and chemical reaction. This process is also an important deformation mechanism in rock salt as is shown in experiments and microstructure research (Urai et al. 1987; Spiers et al. 1990; Spiers and Carter 1998; Martin et al. 1999; Schenk and Urai 2004; Schenk et al. 2006; Ter Heege et al. 2005a, b). The solution-precipitation creep is described as following the Newtonian flow law:

$$\dot{\epsilon}_{PS} = B(\Delta\sigma) = B_0 \exp\left(-\frac{Q}{RT}\right) \left(\frac{\sigma_1 - \sigma_3}{TD^m}\right) \quad (2)$$

and the strain rate $\dot{\epsilon}_{PS}$ is dependent on the grain size D ; $B = B_0 \exp(-Q/TD^m)$ is the viscosity of the salt; and B_0 is a material parameter. The order m influences the strain rate which is dependent on the grain size. Finally, if the dislocation creep and pressure solution creep act simultaneously, the total strain rate is the sum of the two strain rates:

$$\dot{\epsilon} = \dot{\epsilon}_{DC} + \dot{\epsilon}_{PS} \quad (3)$$

Halite rheology is mainly dominated by two main models of the deformation mechanisms in laboratory experiments (Eqs. 1 and 2). These are dislocation creep and solution-precipitation creep. One (pressure solution creep) corresponds to Newtonian viscous rheology with a viscosity dependent on grain size and temperature, the other (dislocation creep) corresponds to the power law creep with a high stress exponent, here creep is mainly temperature-dependent. Based on the deformation mechanisms of rock salt, modelers can choose an effective viscosity which is an implementation of power law creep, making a combination of viscosity associated with both dislocation and solution-precipitation creep (a similar approach is used in many other papers by the salt tectonics modeling community such as van Keken et al. 1993; Koyi 2001; Ings and Beaumont 2010).

Two important differences between Eqs. (1) and (2) are the power order relevant to the influence of stress on strain rate ($n = 1$ for solution-precipitation creep or pressure solution while $n > 1$ for dislocation creep) and secondly the dependence of strain rate on grain size. What needs to be pointed out is that the steady-state creep process is mainly discussed because it is dominant during salt deformation under the long-term conditions.

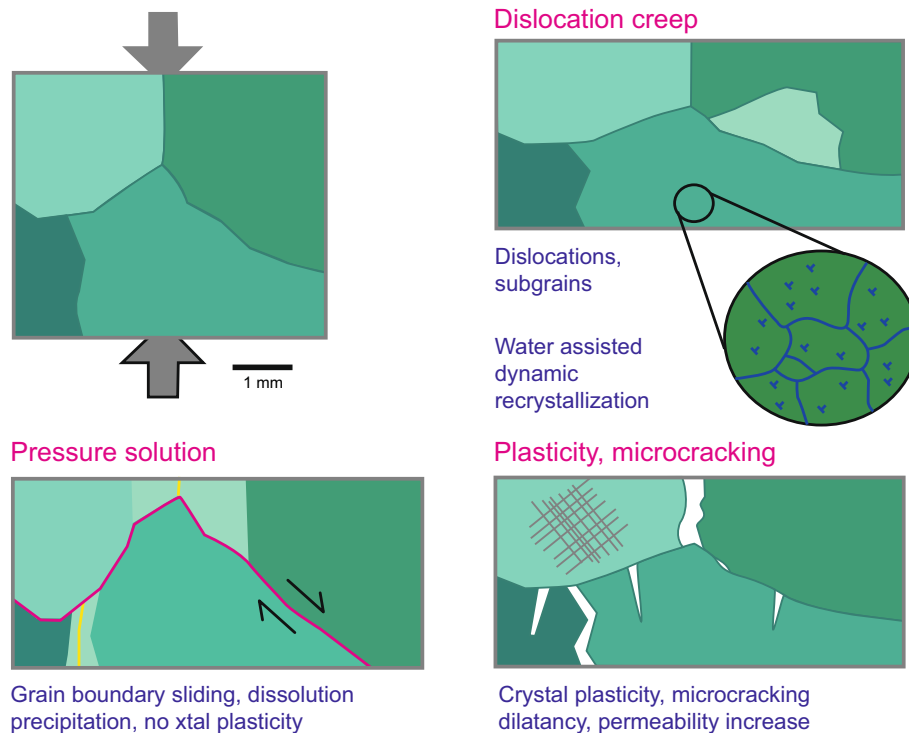


Fig. 1 Deformation mechanisms of rock salt at 20–200 °C. The crystals with different orientations are represented by different green shades (Urai and Spiers 2007)

3 Creep mechanisms at high stresses

3.1 Creep experiments of rock salt at 20–200 °C

Salt flow or halokinesis often occurs at temperatures ranging from 20 to 200 °C. Salt deformation at those temperatures has been widely investigated in laboratories (Heard 1972, 1986; Hansen 1979, Wawersik and Hannum 1980; Wawersik and Zeuch 1984, 1986; Hansen and Carter 1984; Wawersik 1985; Senseny 1988; DeVries 1988; Spiers et al. 1990; Wawersik and Zimmerer 1994; Weidinger et al. 1997; Yang et al. 1999; Hunsche and Hampel 1999; Peach and Spiers 2001; Hunsche et al. 2003, Ter Heege et al. 2005a, b; Schoenherr et al. 2007). The purpose of collecting the experimental data is to provide a basis for deformation modeling and to discuss the influence of different physical parameters on creep properties. The data in Figs. 2 and 3 show the relationship between the strain rate and differential stress during steady-state creep of rock salt from different areas such as Asse, Avery Island, Gorleben, South Oman, and synthetic samples. Two main relationships can be observed, one is between the strain rate and the differential stress (Fig. 2) follows the power law equation which is relevant to dislocation creep, while the other relation (Fig. 3) follows the Newtonian equation which is relevant to pressure solution creep.

3.2 The analysis of the database of laboratory results

It is clearly demonstrated in Fig. 2 that the relation between the strain rate and the differential stress in these experiments is controlled by the power law equation with the power order 5 which is relevant to dislocation creep when the salt deforms at 20–200 °C (Heard 1972; Wawersik and Hannum 1980; Hansen and Carter 1984; DeVries 1988; Weidinger et al. 1997; Hunsche and Hampel 1999; Hunsche et al. 2003). We can see that salt rheology is strongly dependent on temperature, and higher temperature leads to higher strain rate. For every 50 °C increase in temperature, the range of the strain rate varies by around 1.5–2 orders of magnitude for each differential stress. One important thing is that, due to the limited time length in laboratory experiments and strong dependence of grain size and loss of water content, solution-precipitation creep is not often observed in experimental results. The power law related to dislocation creep is considered as engineering creep (Cristescu and Hunsche 1988; Hunsche and Hampel 1999; Fossum and Fredrich 2002).

Some experiments with synthetic samples, for instance, fine grained wet halite also show that solution-precipitation creep controls salt rheology (Urai et al. 1986; Spiers et al. 1990; Spiers and Brzesowsky 1993; Renard et al.

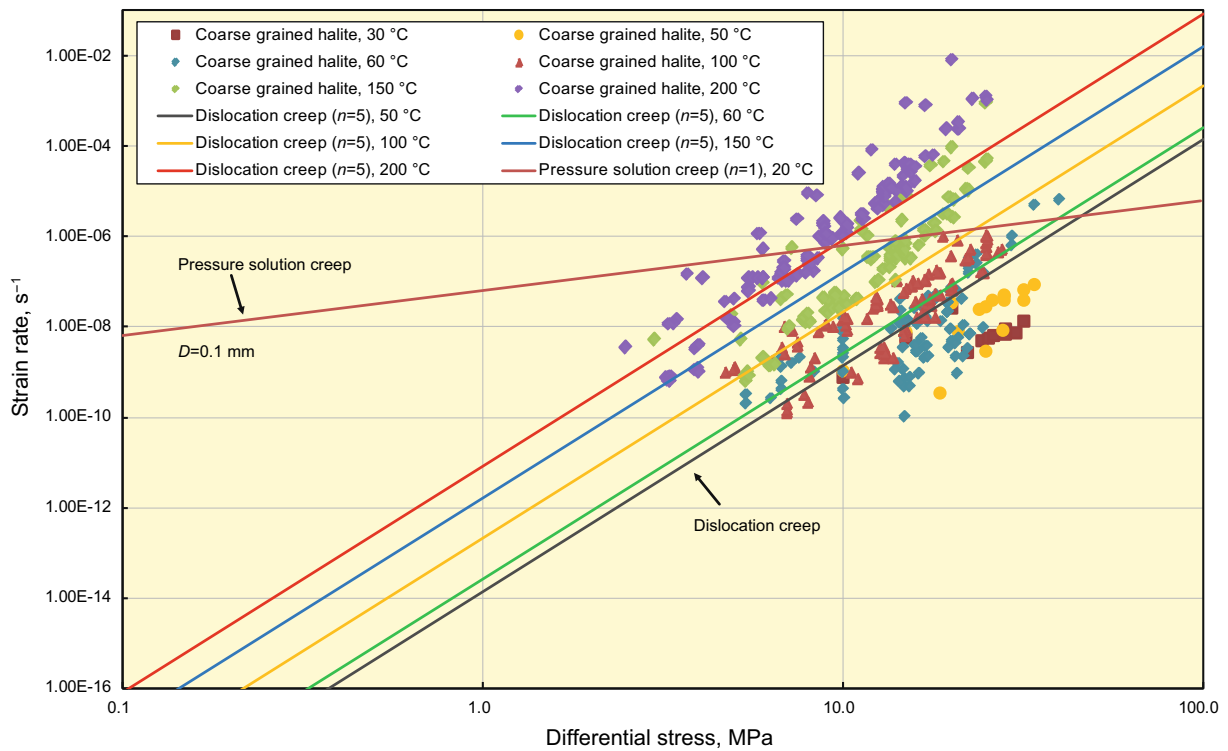


Fig. 2 Strain rate versus differential stress of coarse grain halite at 30–200 °C

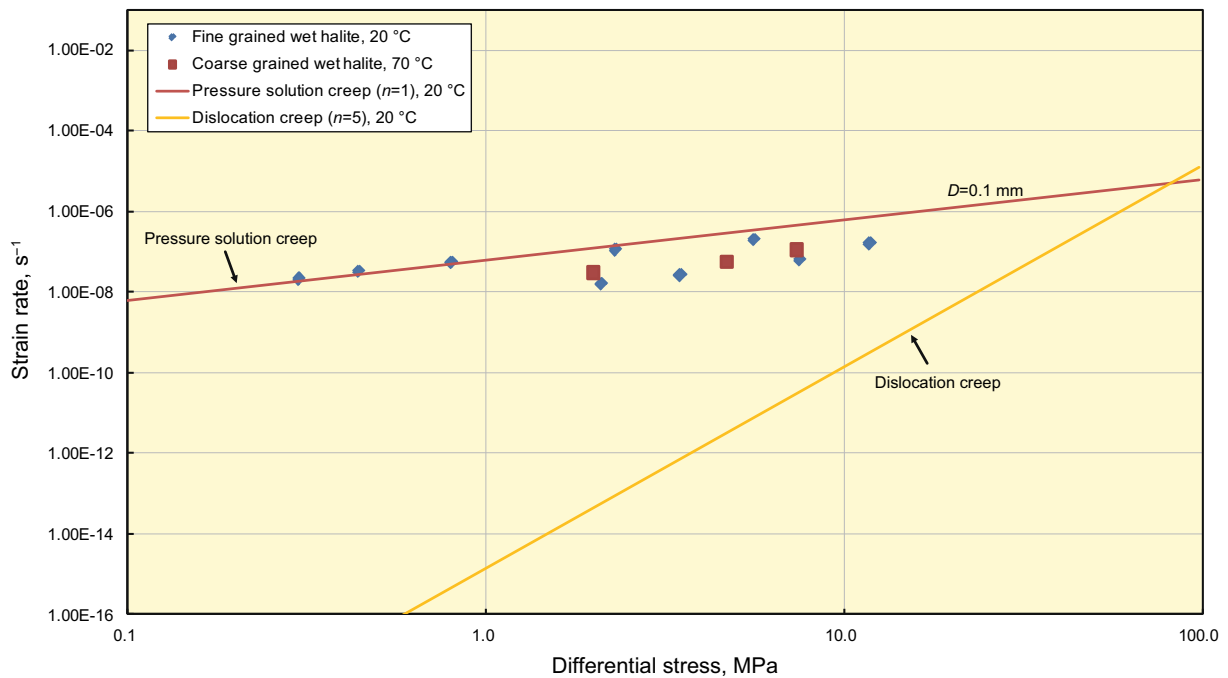


Fig. 3 Strain rate versus differential stress of fine and coarse grain wet halite at 20 and 70 °C

2002, 2004). The data in Fig. 3 show that the salt rheology is dependent on three important factors for wet halite deformation. These are grain size, water content and temperature. The creep strain rate of fine grained wet halite at

20 °C is above 10⁻⁸ s⁻¹ and similar to the one of coarse grained wet halite at 70 °C.

Moreover, solution-precipitation creep is observed in some experiments (where the period of the experiment lasts

more than one year) on coarse grained natural rock salt at low stresses (Bérest et al. 2005). For natural rock salt, solution-precipitation creep has an important influence on the strain rate, and it cannot be neglected. Previous research shows that solution-precipitation creep and dislocation creep occur at the same time and both of them control salt creep. Due to time scale constraints in experiments, it is rather difficult to measure the deformation process with the strain rate below 10^{-9} s^{-1} , in Figs. 2 and 3 we put two creep equations not only for comparison but also as an extrapolation of the data which were observed in experiments. The two creep equations and the rheological parameters A_0 and B_0 are based on the experiments of Spiers et al. (1990) and Wawersik and Zeuch (1986).

The rheological parameters for dislocation creep (Eq. 1) and pressure solution creep (Eq. 2) are listed in Table 1.

4 Numerical simulation of triaxial experiments

In the laboratory, the principal experimental approach is to apply uniaxial or triaxial tensile and compressive loading on a rock salt sample which is drilled from core from salt structures in order to investigate mechanical behavior (for example, the relation between stress and strain or strain rate). In order to prepare for salt tectonics modeling, we develop a numerical model of a triaxial creep experiment of rock salt to verify the specific model using the Abaqus package on salt deformation and evaluate the error due to the boundary conditions in real situations.

The height of the cylindrical sample is 20 cm, and the radius of the cross section is 5 cm (Figs. 4, 5). Table 1 shows the rheological parameters. As a simplified way, we use an axially symmetric model in Abaqus. The loading on

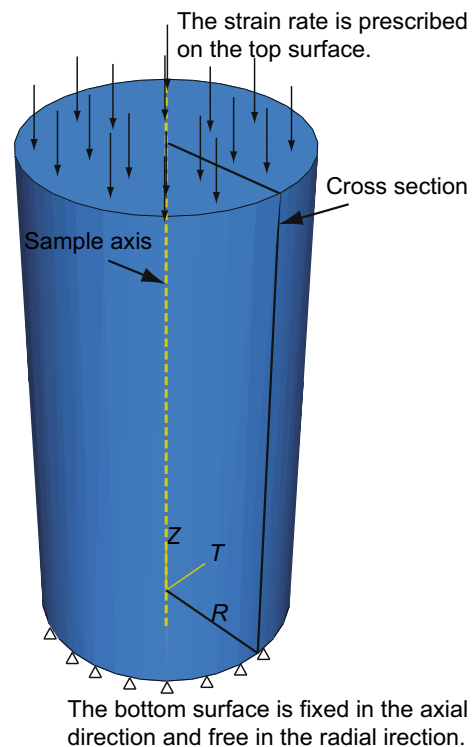


Fig. 4 Cylindrical sample with free boundary conditions in the radial direction

the sample is differential stress $\sigma_1 - \sigma_3$ (σ_1 and σ_3 are two principal stresses in the triaxial experiment). Considering the influence of boundary friction, we simulate two extreme cases, one is radial-free boundary conditions (frictionless) and the other is radial fixed boundary conditions (maximum friction). Two assumptions are taken into consideration, one is the volume which is not changed

Table 1 Material and geometry of rock salt samples in experiments

	Salt A: pressure solution creep (Newtonian flow)	Salt B: dislocation creep (non-Newtonian flow)
A_0 , $\text{MPa}^{-5} \text{ s}^{-1}$	—	7.26×10^{-6}
B_0 , $\text{MPa}^{-1} \text{ s}^{-1}$	4.70×10^{-4}	—
Q , J/mol	24,530	53,920
R , J/mol	8.314	8.314
T , K	323	293
n	1	5
m	3	—
Density ρ , kg/m^3	2200	2200
Young's modulus E , GPa	10	10
Poisson's ratio ν	0.4	0.4
Sample height, cm	20	20
Sample radius, cm	5	5
Reference	Spiers et al. (1990)	Wawersik and Zeuch (1986)

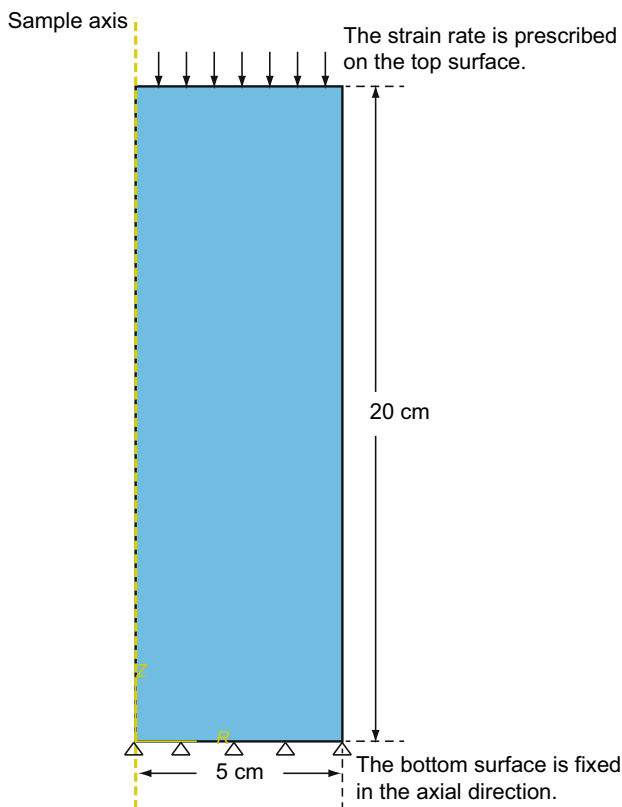


Fig. 5 Half cross section from the cylindrical sample, the yellow line is the sample axis, the bottom surface is fixed in the axial direction and free in the radial direction, the top surface is prescribed by the strain rate in the axial direction and free in the radius direction

during the compression, (incompressibility) and the second one is homogeneous material.

4.1 Simulation of the triaxial creep experiment on a sample with free boundary conditions in the radial direction

In order to obtain the value of differential stress, we calculate the total force $\sum F$ on the top boundary, and then, the total force is divided by the area of the cross section which is due to the radial expansion of the sample as a function of time. We keep the vertical displacement rate on the top surface constant and choose free radial movement on the boundary. On the bottom surface, it is fixed perpendicular to the boundary on the bottom, i.e., no radial movement at one corner and no axial movement at the bottom. For the free radial-movement boundary condition, the homogeneous sample is applied to a uniform displacement rate on the top boundary so that the deformation is also homogeneous. The area of the cross section is:

$$A(t) = \pi[R(t)]^2 = \pi[R_i + u_x(t)]^2 \tag{4}$$

where $A(t)$ is the cross-sectional area; $R(t)$ is the radius of the cylindrical sample; R_i is the initial radius of the sample;

u_x is the displacement in the radial direction. The differential stress $\sigma_1 - \sigma_3$ in the numerical simulation can be confirmed:

$$\sigma(t) = \frac{\sum F}{A(t)} \tag{5}$$

where $\sigma(t)$ is the differential stress; $\sum F$ is the total force acting on the cross section.

4.2 Simulation of the triaxial creep experiment on the sample with fixed boundary conditions in the radial direction

Boundary conditions are fixed perpendicular to the boundary on the bottom and the sides, i.e., no radial movement on the top and bottom edges and no axial movement at the bottom. On the top surface, the vertical displacement rate is applied in the axial direction, and the horizontal displacement in the radial direction is fixed. For the fixed radial-movement boundary condition, heterogeneous deformation occurs due to the fixed boundary condition. The average area of the cross section which is equal to the volume over the length:

$$A(t) = \frac{V}{l(t)} = \frac{V}{l_o \left(1 - \frac{u(t)\Delta t}{l_o}\right)} = \frac{A_o}{1 - \epsilon_{yy}} \tag{6}$$

where $l(t)$ is the length of the cylindrical sample; V is the volume of the sample; A_o is the original area of the cross section, l_o is the original length of the cylindrical sample; and $u(t)$ is the displacement rate; ϵ_{yy} is the strain in the longitudinal direction. The stress is calculated through the total force $\sum F$ over the average area of the cross section $A(t)$, as described in Eq. (5).

4.3 Results of numerical modeling

The parameters and results in the models of free boundary conditions, where the power law and Newtonian law creep are used, respectively, are shown in Tables 2 and 3. Meanwhile, the parameters and results for validations for dislocation creep and solution-precipitation creep in the models of the fixed boundary condition are shown in Tables 4 and 5, respectively.

As we know, the stages of creep include the initial stage called primary creep and the second stage called steady-state creep. In the primary creep stage, the strain rate gradually decreases from a relatively high value. In the steady-state creep stage, the strain rate reaches an almost constant value. The creep strain rate means the rate in the steady-state creep stage. The relation between the differential stress and the creep strain rate can be described as

Table 2 Test parameters and the results of the differential stress (dislocation creep and free radial boundary condition)

	Vertical displacement on the top surface, cm	Total deformation time, s	Strain rate, s^{-1}	Stress $\sigma_1 - \sigma_3$, MPa
Strain rate 1	2.48	1.0E+19	1.41E−20	0.10
Strain rate 2	2.48	1.0E+14	1.41E−15	1.00
Strain rate 3	2.42	1.0E+12	1.37E−13	2.50
Strain rate 4	2.37	1.0E+10	1.34E−11	6.25
Strain rate 5	2.30	1.0E+08	1.30E−09	15.60
Strain rate 6	2.26	1.0E+06	1.27E−07	39.00
Strain rate 7	2.22	1.0E+04	1.25E−05	97.60

Table 3 Test parameters and the results of the differential stress (solution-precipitation creep and free radial boundary condition)

	Vertical displacement on the top surface, cm	Total deformation time, s	Strain rate, s^{-1}	Stress $\sigma_1 - \sigma_3$, MPa
Strain rate 1	2.54	1.2E+13	1.21E−14	0.10
Strain rate 2	2.54	1.2E+12	1.21E−13	1.00
Strain rate 3	2.16	4.0E+11	3.02E−13	2.50
Strain rate 4	2.40	1.8E+11	7.56E−13	6.25
Strain rate 5	2.34	7.0E+10	1.89E−12	15.60
Strain rate 6	2.49	3.0E+10	4.72E−12	39.00
Strain rate 7	2.13	1.0E+10	1.18E−11	97.60

Table 4 Test parameters and the results of the differential stress (dislocation creep and fixed radial boundary condition)

	Vertical displacement on the top surface, cm	Total deformation time, s	Strain rate, s^{-1}	Stress $\sigma_1 - \sigma_3$, MPa
Strain rate 1	2.48	1.0E+19	1.41E−20	0.10
Strain rate 2	2.48	1.0E+14	1.41E−15	1.03
Strain rate 3	2.42	1.0E+12	1.37E−13	2.58
Strain rate 4	2.37	1.0E+10	1.34E−11	6.44
Strain rate 5	2.30	1.0E+08	1.30E−09	16.06
Strain rate 6	2.26	1.0E+06	1.27E−07	40.12
Strain rate 7	2.22	1.0E+04	1.25E−05	100.13

Table 5 Test parameters and the results of differential stress (solution-precipitation creep and fixed radial boundary condition)

	Vertical displacement on the top surface, m	Total deformation time, s	Strain rate, s^{-1}	Stress $\sigma_1 - \sigma_3$, MPa
Strain rate 1	2.54	1.2E+13	1.21E−14	0.11
Strain rate 2	2.54	1.2E+12	1.21E−13	1.09
Strain rate 3	2.16	4.0E+11	3.02E−13	2.72
Strain rate 4	2.40	1.8E+11	7.56E−13	6.78
Strain rate 5	2.34	7.0E+10	1.89E−12	16.90
Strain rate 6	2.49	3.0E+10	4.72E−12	42.12
Strain rate 7	2.13	1.0E+10	1.18E−11	105.28

Eqs. (1) or (2). In the numerical simulation, we apply the elastic law and power law equations (the steady-state creep equations) on the rock salt sample.

We can obtain the relationship between the differential stress and the strain when dislocation creep dominates ($n = 5$) and evaluate the friction boundary effect in the

experiment. We can obtain the relation between the differential stress and the strain rate in the steady-state creep stage and make a comparison between the numerical and experimental results. In Fig. 6, we can see that the thick dots represent the differential stress with the fixed boundary condition. The thin dots represent the differential stress with the free boundary condition. The homogeneous deformation results in a constant stress in the steady state. When the strain is the same, the differential stress with the radial fixed boundary condition is higher than the one with the radial-free boundary condition.

From the stress–strain curve in Fig. 7, we can see the mechanical behavior of rock salt includes elastic and steady-state creep processes. However, it is obvious there is a ‘pseudo’-primary creep between the elastic and steady-state creep stages. In the numerical model, we do not apply primary creep in the material property. It is because creep which leads to stress relaxation can occur even when the elastic strength is not reached after the loading is applied for a short period time. In Fig. 7, we can see the relation between the differential stress and the strain when solution-precipitation creep dominates ($n = 1$). The thick dots represent the differential stress with the fixed boundary condition. The thin dots represent the differential stress with the free boundary condition. The differential stress increases slowly because in reality the top surface displacement velocity is constant and the strain rate increases slowly. The change in stress is very relevant to the slow increase in the strain rate when the Newtonian creep law ($n = 1$) dominates.

Figure 8 shows the diagram of the differential stress and strain rate, and it summarizes low-temperature laboratory data and numerical simulation results. The broken line is extrapolation of the dislocation creep equation, taking $n = 5$. The blue and red dots show the results of the relation between the differential stress and the strain rate for $n = 5$ and $n = 1$, respectively, from the numerical simulation with free x -movement boundary (the frictionless boundary condition) of the cylindrical sample. We can see that the numerical solutions fit the experimental results quite well. Although from the numerical results the relation between stress and strain has a small difference from the theoretical situation, the relation between the strain rate and the differential stress with the free boundary condition matches the theoretical situation very well. This shows that for the steady-state creep the numerical solution is in a good agreement with the experimental result despite a ‘pseudo-primary creep’ between the elastic and steady-state creep stages. Therefore, the numerical result of the parameter A and the power order n (Eq. 1) achieved from the free radial-movement boundary condition can be thought of as the correct rheology.

5 Creep mechanisms at low stresses

Some experiments with synthetic samples show that solution-precipitation creep can play a role at low stresses (Spiers et al. 1990). However, as an important extrapolation of laboratory data, it is necessary to study the rock salt

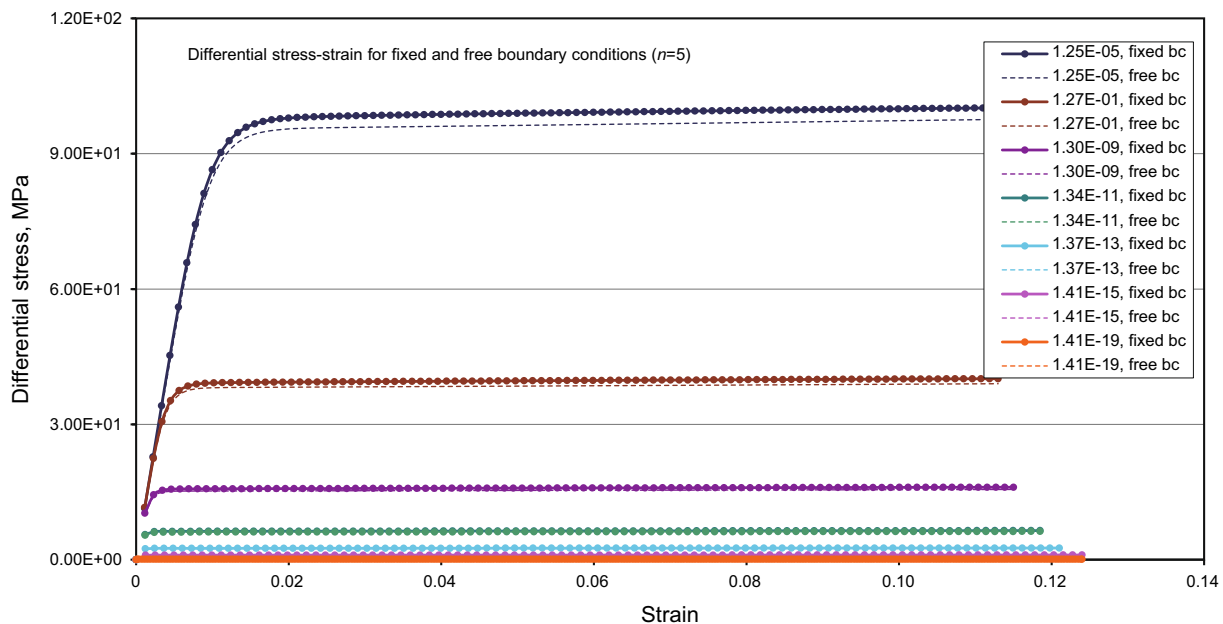


Fig. 6 Differential stress and strain in the y direction for fixed and free boundary conditions ($n=5$)

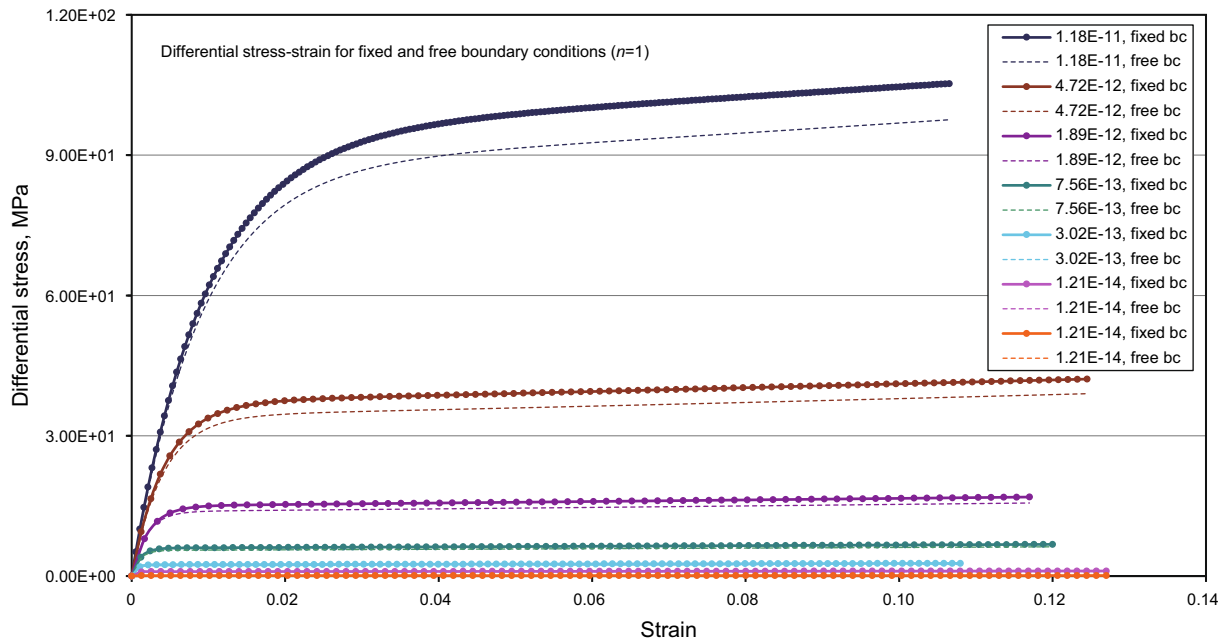


Fig. 7 Differential stress and strain in the y direction for fixed and free boundary conditions ($n=1$)

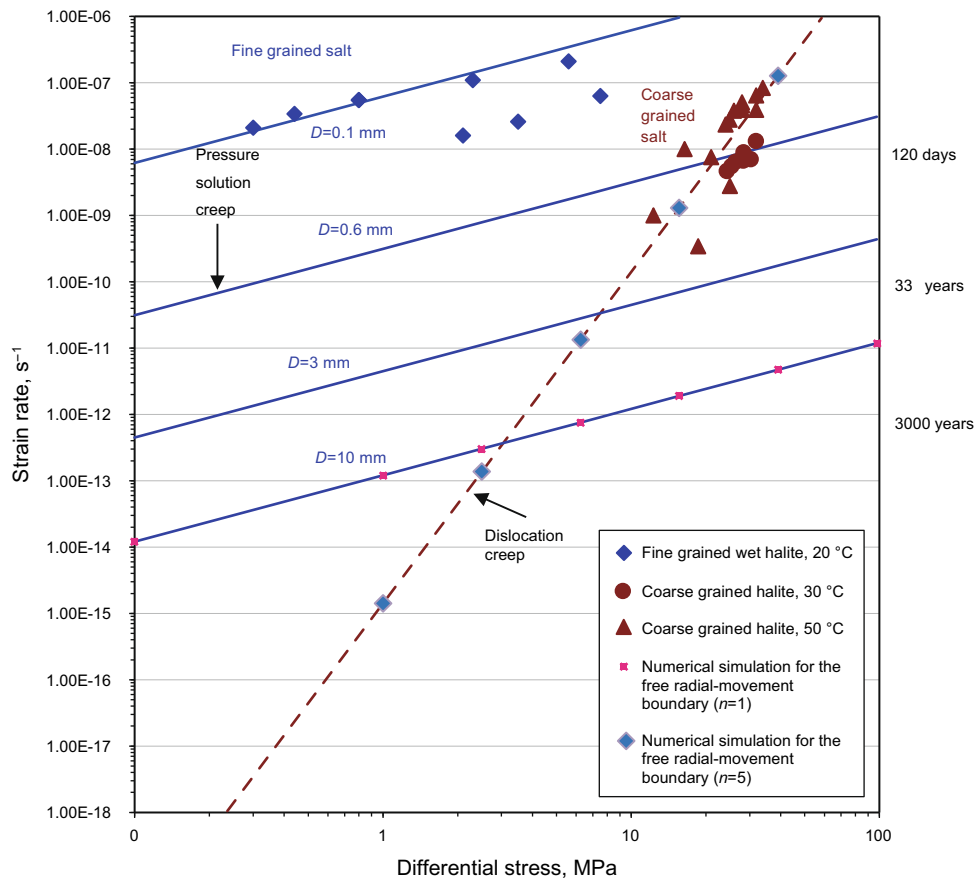


Fig. 8 Differential stress versus strain rate diagram. *Solid lines* are the pressure solution creep for fine and coarse grain sizes at room temperature. The *broken line* is the extrapolation of the dislocation

creep. The *red and blue dots* represent numerical results with free radial-movement boundary condition (modified from Urai and Spiers 2007)

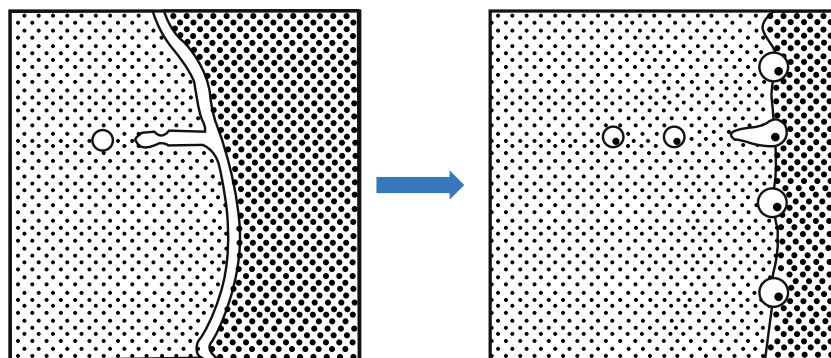


Fig. 9 Rock salt grain boundaries will tend to heal with a decrease in differential stress (Drury and Urai 1990)

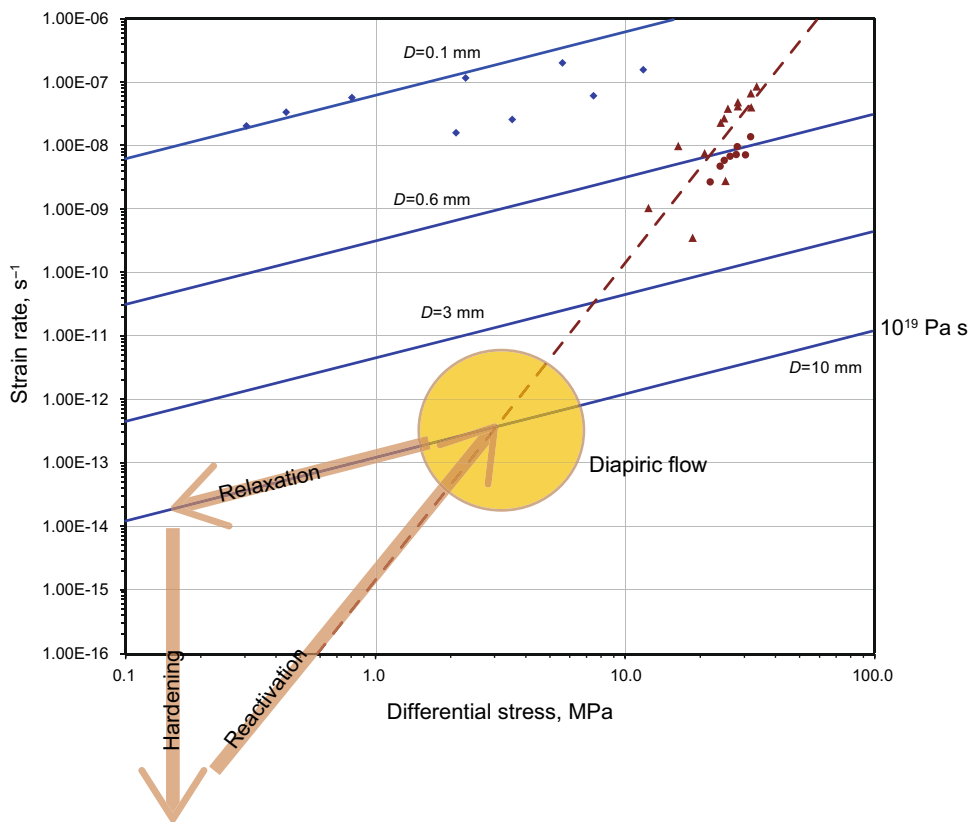


Fig. 10 Two deformation mechanisms at differential stresses around and below 2 MPa (Urai et al. 2008)

deformation in nature in order to observe detailed information for deformation mechanisms (Schlöder and Urai 2005; Schlöder et al. 2008). For creep of salt under high differential stresses, for example, 2.0 MPa, which is in agreement with many studies which used subgrain size piezometry on salt deformed by a combination of dislocation creep and pressure solution creep. The effective viscosity is a permissible model, because the dynamic recrystallization tends to bring the contributions of dislocation creep and pressure solution creep into balance and grain boundaries are mobile (De Bresser et al. 2001). However, the observation of rock salt deformation in the

natural laboratory through microstructural research provides the important information for the differential stress smaller than 2.0 MPa. Under this differential stress, the dynamic recrystallization changes the grain size and it contributes to the balance between the dislocation and pressure solution creep controlling rock salt deformation. If the differential stress is much lower, grain boundaries tend to heal or neck driven by interfacial energy, then the grain boundaries immobile (Fig. 9). Pressure solution creep is switched off, and deformation can only proceed by dislocation creep, at dramatically lower strain rates. In other words, the effective viscosity under these low differential

stress values is many orders of magnitude higher. A more detailed recent review of these issues is Urai et al. (2008). In the initial stage of salt tectonics, the differential stresses in salt are very low, and recent studies suggest that under these conditions pressure solution creep in the salt should be inactive and salt deforms under the control of dislocation creep ($n = 5$). A related issue is raised by the observation that anhydrite–dolomite stringers do not sink through salt over long geologic periods (van Gent et al. 2011; Burchardt et al. 2011). In conclusion, the strain rates are similar at a differential stress around 2 MPa during salt tectonics under the controls of both dislocation creep and pressure solution creep. However, the pressure solution creep is inactive and switched off at lower stress below 2 MPa after salt tectonics stops. During and after salt tectonics, dislocation creep is always active and dominant for the rock salt deformation (Fig. 10).

6 Conclusions

The creep equations controlled by microstructure deformation mechanisms are the foundation of modeling rock salt creep properties under long-term conditions, and they are useful for salt tectonics modeling and salt mining engineering. In this paper, we summarized the research findings on creep controlled by two deformation mechanisms (dislocation creep and solution-precipitation creep) and built a database for rock salt rheology at 20–200 °C. Various rock salt has different water contents in the pore and grain boundaries, which strongly affects the rheological behavior. The temperature also plays an important role in rock salt deformation. Moreover, we modeled creep behavior of rock samples at various strain rates under the control of two deformation mechanisms. The numerical model in the Abaqus package can simulate the real triaxial experiment and can be used for salt tectonics modeling. The numerical simulation can also evaluate the effect of boundary conditions on the creep property. Finally, both deformation mechanisms lead to a similar strain rate during salt tectonics, and the pressure solution creep is inactive at a low stress after salt tectonics. Combined with experimental results in laboratories and microstructure research as the reliable exploration of experimental results, we conclude that rock salt rheology can be simplified to dislocation creep corresponding to power law creep ($n = 5$) with the appropriate material parameters in the salt tectonic modeling.

Acknowledgments We would like to thank Steffen Abe, Lars Reuning and Frank Strozyk for their contributions to the work. We also thank RWTH Aachen University and China University of Petroleum for the support of the work and Prof. Zhang Guangqing and the Department of Engineering Mechanics. The research is funded by the startup project of China University of Petroleum, Beijing (No.

2462014YJRC041) and supported by Science Foundation of China University of Petroleum, Beijing (No. C201601).

Open Access This article is distributed under the terms of the Creative Commons Attribution 4.0 International License (<http://creativecommons.org/licenses/by/4.0/>), which permits unrestricted use, distribution, and reproduction in any medium, provided you give appropriate credit to the original author(s) and the source, provide a link to the Creative Commons license, and indicate if changes were made.

References

- Aubertin M, Gill DE, Ladanyi B. An internal variable model for the creep of rocksalt. *Rock Mech Rock Eng.* 1991;24(2):81–97. doi:10.1007/BF01032500.
- Bérest P, Blum PA, Charpentier JP, et al. Very slow creep tests on rock samples. *Int J Rock Mech Min Sci.* 2005;42(4):569–76.
- Brouard B, Bérest P. A tentative classification of salts according to their creep properties. In: *Proceedings of SMRI spring meeting, New Orleans; 1998.* pp. 18–38.
- Burchardt S, Koyi H, Schmeling H. Strain pattern within and around denser blocks sinking within Newtonian salt. *J Struct Geol.* 2011;33(2):145–53. doi:10.1016/j.jsg.2010.11.007.
- Carter NL, Hansen FD. Creep of rocksalt. *Tectonophysics.* 1983;92(4):275–333. doi:10.1016/0040-1951(83)90200-7.
- Carter NL, Horseman ST, Russell JE, Handin J. Rheology of rocksalt. *J Struct Geol.* 1993;15(9–10):1257–71. doi:10.1016/0191-8141(93)90168-A.
- Chemia Z, Koyi H, Schmeling H. Numerical modeling of rise and fall of a dense layer in salt diapirs. *Geophys J Int.* 2008;172:798–816. doi:10.1111/j.1365-246X.2007.03661.x.
- Chemia Z, Koyi H. The control of salt supply on entrainment of an anhydrite layer within a salt diapir. *J Struct Geol.* 2008;30(9):1192–200. doi:10.1016/j.jsg.2008.06.004.
- Chemia Z, Schmeling H. The effect of the salt viscosity on future evolution of the Gorleben salt diapir, Germany. *Tectonophysics.* 2009;473(3–4):446–56. doi:10.1016/j.tecto.2009.03.027.
- Cristescu ND, Hunsche U. *Time effects in rock mechanics.* New York: Wiley; 1988. p. 342.
- Cristescu ND. A general constitutive equation for transient and stationary creep of rocksalt. *Int J Rock Mech Min Sci Geomech Abstr.* 1993;30(2):125–40.
- Cristescu ND. Evolution of damage in rocksalt. In: *Mechanical behavior of salt.* Trans Tech Publications, Series on Rock and Soil Mechanics, Clausthal-Zellerfeld. 1998; 22:131–42.
- De Bresser JHP, Ter Heege JH, Spiers CJ. Grain size reduction by dynamic recrystallization: can it result in major rheological weakening? *Int J Earth Sci.* 2001;90:28–45. doi:10.1007/s005310000149.
- De Meer S, Spiers CJ, Peach CJ, et al. Diffusive properties of fluid-filled grain boundaries measured electrically during active pressure solution. *Earth Planet Sci Lett.* 2002;200(1–2): 147–57. doi:10.1016/S0012-821X(02)00585-X.
- Deng JG. Calculation method of mud density to control borehole closure. *Chin J Rock Mech Eng.* 1997;16(6):522–8 (in Chinese).
- DeVries KL. *Viscoplastic laws for Avery Island salt.* Report for Stone Webster, RSI-0333, RE/SPEC, Inc., Rapid City, S.D. 1988.
- Drury M, Urai J. Deformation-related recrystallization processes. *Tectonophysics.* 1990;172:235–53. doi:10.1016/0040-1951(90)90033-5.
- Franssen RCMW. The rheology of synthetic rocksalt in uniaxial compression. *Tectonophysics.* 1994;233(1–2):1–40. doi:10.1016/0040-1951(94)90218-6.

- Fossum AF, Fredrich JT. Salt mechanics primer for near-salt and sub-salt deepwater Gulf of Mexico Field Developments. Sandia report, SAND2002–2063. (2002).
- Gemmer L, Ings SJ, Medvedev S, et al. Salt tectonics driven by differential sediment loading: stability analysis and finite-element experiments. *Basin Res.* 2004;16(2):199–218. doi:10.1111/j.1365-2117.2004.00229.x.
- Hampel A, Hunsche U, Weidinger P, et al. Description of the creep of rock salt with the composite model—II. steady state creep. In: Aubertin M, Hardy H Jr., editors. The mechanical behavior of salt IV. Trans Tech Publications, Clausthal. 1998. pp. 287–99.
- Hampel A, Schulze O. The composite dilatancy model: a constitutive model for the mechanical behavior of rock salt. In: Proceeding of 6th conference of the mechanical behavior of salt understanding of THMC processes in salt; 2007. pp. 99–107.
- Hansen FD. Creep behavior of bedded salt from Southeastern New Mexico at elevated temperatures. Report SAND 9-7030. Sandia National Laboratories. 1979.
- Hansen FD, Carter NL. Creep of Avery Island rocksalt. In: Proceedings of the first conference on mechanical behavior of salt, Clausthal-Zellerfeld, Germany. Trans Tech Publications; 1984. pp. 53–69.
- Haupt M, Schweiger HF. Development of a constitutive model for rock salt based on creep and relaxation tests. *Comput Geotech.* 1989;7(4):346.
- Heard HC. Steady-state flow in polycrystalline halite at pressure of 2 kilobars. In: Heard HC, Borg IY, Carter NL, Raleigh CB, editors. Flow and fracture of rocks. AGU Geophysical Monograph Series. 1972;16:191–210. doi:10.1029/GM016p0191.
- Heard HC, Ryerson FJ. Effect of cation impurities on steady-state flow of salt. In: Hobbs BE, Heard HC, editors. Mineral and rock deformation: laboratory studies. AGU Geophysical Monograph Series. 1986;36:99–115. doi:10.1029/GM036p0099.
- Hunsche U, Hampel A. Rock salt—the mechanical properties of the host rock material for a radioactive waste repository. *Eng Geol.* 1999;52(3–4):271–91. doi:10.1016/S0013-7952(99)00011-3.
- Hunsche U, Schulze O, Walter F, et al. Projekt Gorleben: Thermo-mechanisches Verhalten von Salzgestein. 2003. (in German).
- Ings SJ, Beaumont C. Shortening viscous pressure ridges, a solution to the enigma of initiating salt ‘withdrawal’ minibasins. *Geology.* 2010;38(4):339–42. doi:10.1130/G30520.1.
- Jin J, Cristescu ND. An elastic/viscoplastic model for transient creep of rock salt. *Int J Plast.* 1998;14(1–3):85–107. doi:10.1016/S0749-6419(97)00042-9.
- Koyi H. Salt flow by aggrading and prograding overburdens. In: Alsop I, Blundell D, Davison I, editors. Salt tectonics. Geological Society, London, Special Publications. 1996;100(1):243–58.
- Koyi H. The shaping of salt diapirs. *J Struct Geol.* 1998;20(4):321–38. doi:10.1016/S0191-8141(97)00092-8.
- Koyi H. Modeling the influence of sinking anhydrite blocks on salt diapirs targeted for hazardous waste disposal. *Geology.* 2001;29(5):387–90. doi:10.1130/0091-7613(2001).
- Li S, Abe S, Reuning L, Becker S, Urai JL, Kukla PA. Numerical modeling of the displacement and deformation of embedded rock bodies during salt tectonics—a case study from the South Oman Salt Basin. In: Alsop I, editors. Salt tectonics, sediments and prospectivity. Geological Society Special Publication. 2012a;363:503–20. doi:10.1144/SP363.24.
- Li S, Strozzyk F, Abe S, van Gent H, Kukla P, Urai JL. A method to evaluate long-term rheology of Zechstein Salt in the Tertiary. In: Berest P, Ghoreychi M, Hadj-Hassen F, Tijani M, editors. Mechanical behavior of salt VII. Taylor & Francis Group, London; 2012b. pp. 215–20.
- Li SQ, Feng L, Tang PC, Rao G, Bao YH. Calculation of depth to detachment and its significance in the Kuqa Depression: a discussion. *Pet Sci.* 2009;6:17–20. doi:10.1007/s12182-009-0003-2.
- Liang WG, Zhao YS. Investigation on carbon dioxide geological sequestration in salt caverns. *Chin J Undergr Space Eng.* 2007;2:1545–50 (in Chinese).
- Martin B, Röller K, Stoeckert B. Low-stress pressure solution experiments on halite single-crystals. *Tectonophysics.* 1999;308(3):299–310. doi:10.1016/S0040-1951(99)00112-2.
- Munson DE. Constitutive model for the low temperature creep of salt (with application to WIPP). Technical report, SAND79-1853. Sandia National Laboratories, Albuquerque, NM. 1979.
- Munson DE. Constitutive model of creep in rock salt applied to underground room closure. *Int J Rock Mech Min Sci.* 1997;34(2):233–47. doi:10.1016/S0148-9062(96)00047-2.
- Ottosen NS. Viscoelastic-viscoplastic formulas for analysis of cavities in rock salt. *Int J Rock Mech Min Sci Geomech Abstr.* 1986;23(3):201–12. doi:10.1016/0148-9062(86)90966-6.
- Peach CJ, Spiers CJ. Influence of crystal plastic deformation on dilatancy and permeability development in synthetic salt rock. *Tectonophysics.* 1996;256(1–4):101–28. doi:10.1016/0040-1951(95)00170-0.
- Peach CJ, Spiers CJ, Trimby PW. Effect of confining pressure on dilatation, recrystallization, and flow of rock salt at 150 °C. *J Geophys Res.* 2001;106:13315–28. doi:10.1029/2000JB900300.
- Poliakov ANB, Podladchikov Y, Talbot C. Initiation of salt diapirs with frictional overburdens: numerical experiments. *Tectonophysics.* 1993;228:99–210. doi:10.1016/0040-1951(93)90341-G.
- Renard F, Dysthe D, Feder J, Jamtveit B. Healing of fluid-filled microcracks. In: Proceedings of the second Biot conference on poromechanics. 2002; pp. 925–31.
- Renard F, Bernard D, Thibault X, Boller E, et al. Synchrotron 3D microtomography of halite aggregates during experimental pressure solution creep and evolution of the permeability. *Geophys Res Lett.* 2004;31:L07607. doi:10.1029/2004GL019605.
- Rutter EH. Pressure solution in nature, theory and experiment. *J Geol Soc.* 1983;140:725–40. doi:10.1144/gsjgs.140.5.0725.
- Schenk O, Urai JL. Microstructural evolution and grain boundary structure during static recrystallization in synthetic polycrystals of sodium chloride containing saturated brine. *Contrib Miner Pet.* 2004;146:671–82. doi:10.1007/s00410-003-0522-6.
- Schenk O, Urai JL, Piazzolo S. Structure of grain boundaries in wet, synthetic polycrystalline, statically recrystallizing halite—evidence from cryo-SEM observations. *Geofluids.* 2006;6(1):93–104. doi:10.1111/j.1468-8123.2006.00134.x.
- Schlöder Z, Urai JL. Microstructural evolution of deformation-modified primary halite from Hengelo, The Netherlands. *Int J Earth Sci.* 2005;94(5–6):941–56. doi:10.1007/s00410-003-0522-6.
- Schlöder Z, Urai JL, Nolle S, Hilgers C. Solution-precipitation creep and fluid flow in halite: a case study on Zechstein (Z1) rocksalt from Neuhof salt mine (Germany). *Int J Earth Sci.* 2008;97(5):1045–56. doi:10.1007/s00531-007-0275-y.
- Schoenherr J, Schlöder Z, Urai JL, Fokker PA, Schulze O. Deformation mechanisms and rheology of Pre-Cambrian rocksalt from the South Oman Salt Basin. In: Proceedings of the 6th conference on the mechanical behavior of salt—understanding of THMC processes in salt. Hannover, Germany, 22–25 May 2007. pp. 167–73.
- Schultz-Ela DD, Jackson MPA. Evolution of extensional fault systems linked with salt diapirism modeled with finite elements. *AAPG Bull.* 1993;77:179.
- Senseny PE. Creep properties of four rock salts. In: Proceeding of the 2nd conference on mechanical behavior of salt. Trans. Tech. Pub; 1988. pp. 431–44.

- Senseny PE, Hansen FD, Russell JE, Carter NL, Handin JW. Mechanical behaviour of rock salt: phenomenology and micromechanisms. *Int J Rock Mech Min Sci Geomech Abstr.* 1992;29(4):363–78.
- Spiers CJ, Schutjens PMTM, Brzesowsky RH, Peach CJ, Liezenberg JL, Zwart HJ. Experimental determination of constitutive parameters governing creep of rocksalt by pressure solution. In: Knipe RJ, Rutter EH, editors. *Deformation mechanisms, rheology and tectonics.* Geological Society, London, Special Publications. 1990;54(1):215–27. doi:10.1144/GSL.SP.1990.054.01.21.
- Spiers CJ, Brzesowsky RH. Densification behaviour of wet granular salt: theory versus experiment. In: Kakinana H, Hardy HR, Jr, Hoshi T, Toyokura K, editors. *Seventh symposium on salt.* Elsevier Amsterdam, 1993;(1):83–92.
- Spiers CJ, Carter NL. Microphysics of rocksalt flow in nature. In: Aubertin M, Hardy HR, editors. *The mechanical behavior of salt proceedings of the 4th conference,* Trans Tech. Publ. Series on Rock and Soil Mechanics, 1998;22:15–128.
- Tang JP, Wang SQ, Chen M. *Salt-gypsum drilling theory and application.* Beijing: Petroleum Industry Press; 2004 (in Chinese).
- Ter Heege JH, De Bresser JHP, Spiers CJ. Dynamic recrystallization of wet synthetic polycrystalline halite: dependence of grain size distribution on flow stress, temperature and strain. *Tectonophysics.* 2005a;396(1–2):35–57. doi:10.1016/j.tecto.2004.10.002.
- Ter Heege JH, De Bresser JHP, Spiers CJ. Rheological behaviour of synthetic rocksalt: the interplay between water, dynamic recrystallization and deformation mechanisms. *J Struct Geol.* 2005b;27(6):948–63. doi:10.1016/j.jsg.2005.04.008.
- Urai JL, Spiers CJ, Zwart HJ, Lister GS. Weakening of rock salt by water during long-term creep. *Nature.* 1986;324:554–7. doi:10.1038/324554a0.
- Urai JL, Spiers CJ, Peach CJ, Franssen RCMW, Liezenberg JL. Deformation mechanisms operating in naturally deformed halite rocks as deduced from microstructural investigations. *Geol Mijnbouw.* 1987;66:165–76.
- Urai JL, Spiers CJ. The effect of grain boundary water on deformation mechanisms and rheology of rocksalt during long-term deformation. In: Wallner M, Lux K, Minkley W, Hardy H Jr., editors. *Proceeding of the 6th conference of mechanical behavior of salt understanding of THMC processes in salt;* 2007. pp. 149–58.
- Urai JL, Schlöder Z, Spiers CJ, Kukla PA. Flow and transport properties of saltrocks. In: Littke R, Bayer U, Gajewski D, Nelskamp S, editors. *Dynamics of complex intracontinental basins: The Central European Basin System.* Berlin: Springer; 2008. p. 277–90.
- van Gent H, Urai JL, De Keijzer M. The internal geometry of salt structures—a first look using 3D seismic data from the Zechstein of the Netherlands. *J Struct Geol.* 2011;33(2):292–311. doi:10.1016/j.jsg.2010.07.005.
- van Keken PE, Spiers CJ, van den Berg AP, Muyzent EJ. The effective viscosity of rocksalt: implementation of steady-state creep laws in numerical models of salt diapirism. *Tectonophysics.* 1993;225(4):457–76. doi:10.1016/0040-1951(93)90310-G.
- Wawersik WR. Determination of steady state creep rates and activation parameters for rock salt. In: Pineus HJ, Hoskins ER, editors. *Measurement of rock properties at elevated pressures and temperatures,* ASTM STP 869. Philadelphia: American Society for Testing and Materials; 1985. pp. 72–92.
- Wawersik WR, Hannum DW. Mechanical behavior of New Mexico rock salt in triaxial compression up to 200 °C. *J Geophys Res.* 1980;85:891–900. doi:10.1029/JB085iB02p00891.
- Wawersik WR, Zeuch DH. Creep and creep modeling of three domal salts—a comprehensive update. Technical report, SAND84-0568. Sandia National Laboratories, Albuquerque, NM (United States). 1984.
- Wawersik WR, Zeuch DH. Modeling and mechanistic interpretation of creep of rocksalt below 200 °C. *Tectonophysics.* 1986;121(2–4):125–52. doi:10.1016/0040-1951(86)90040-5.
- Wawersik WR, Zimmerer DJ. Triaxial creep measurements on rock salt from the Jennings Dome. Technical report. Louisiana, Borehole LA-1, Core #8*. Technical report, SAND94-1432. Sandia National Laboratories, Albuquerque, NM (United States). 1994.
- Weidinger P, Hampel A, Blum W, Hunsche U. Creep behaviour of natural rock salt and its description with the composite model. *Mater Sci Eng.* 1997;234:646–8. doi:10.1016/S0921-5093(97)00316-X.
- Yang CH, Daemen JJK, Yin JH. Experimental investigation of creep behavior of salt rock. *Int J Rock Mech Min Sci.* 1999;36:233–42. doi:10.1016/S0148-9062(98)00187-9.
- Yang CH, Li YP, Chen F, Shi XL, Qu DA. Advances in researches of the mechanical behaviors of deep bedded salt rocks in China. In: *Proceedings of the 43rd U.S. rock mechanics symposium and 4th U.S.—Canada rock mechanics symposium,* Asheville. 2009.
- Yang HL, Chen M, Zhang GQ. Deformation mechanisms and safe drilling fluids density in extremely thick, salt formations. *Pet Sci.* 2007;4(4):56–61. doi:10.1007/BF03187456.
- Zhang GQ, Chen M, Zhao YB. Study on initiation and propagation mechanism of fractures in oriented perforation of new wells. *Acta Pet Sin.* 2008;29(1):116–9 (in Chinese).
- Zhang GQ, Chen M. Complex fracture shapes in hydraulic fracturing with orientated perforations. *Pet Explor Dev.* 2009;36(1):103–7. doi:10.1016/S1876-3804(09)60113-0 (in Chinese).
- Zhang GQ, Chen M. Dynamic fracture propagation in hydraulic fracturing. *J Pet Sci Eng.* 2010;70(3–4):266–72. doi:10.1016/j.petrol.2009.11.019.